PCCP

Accepted Manuscript

ROYAL SOCIETY OF CHEMISTRY

www.rsc.org/pccp

Physical Chemistry Chemical Physics
CREATED USING THE RSC LaTeX PCCP ARTICLE TEMPLATE – SEE www.rsc.org/electronicfiles FOR DETAILS
ARTICLE TYPE www. rsc.org/xxxxxx | XXXXXXXX

Acoustic dynamics of supercooled indomethacin probed by Brilluoin light scattering.

S. De Panfilis[a], E. A. A. Pogna[b], A. Virga[b] and T. Scopigno[b*]

a Centre for Life Nano Science – IIT@Sapienza, Istituto Italiano di Tecnologia, I-00161 Roma (Italy).
b Dipartimento di Fisica, Universitá di Roma "Sapienza", I-00185 Roma (Italy).

Received Xth XXXXXXXXXX 20XX, Accepted Xth XXXXXXXXX 20XX
First published on the web Xth XXXXXXXXXX 200X
DOI: 10.1039/b000000x

Acoustics dynamics of the molecular glass-former indomethacin (IMC) have been investigated by Brillouin light scattering (BLS) at GHz frequencies. Elastic response of the system has been tracked from the melting temperature down to the glass transition through the supercooled liquid. Both the structural arrest and the vibrational dynamics are described by modeling the experimentally determined dynamic structure factor within the framework of the Langevin equation, through a simplified choice of memory function which allows one to determine sound velocity and acoustic attenuation coefficient as function of temperature. The density fluctuations spectra in the glassy phase, as probed by BLS, are compared with time-domain results from photoacoustics experiments. The arising scenario is discussed in the context of current literature reporting inelastic x-ray scattering and BLS in platelet geometry. The link between the probed elastic properties and the non-ergodicity factor of the glass phase is finally scrutinized.

1 Introduction

Pharmaceutical products must be stable over storage periods of many months, typically several years, and many biomolecules do not possess this long-term stability in the aqueous state at ambient temperature. To attain extended stability at ambient temperature during storage, molecular movement needs to be arrested by vitrification, a method that stops degradation by transforming a liquid into a highly immobile, non-crystalline, amorphous solid state[1]. The glass-former system below its glass transition temperature (T_g) is stable due to the immobilization of the reactive entity. Moreover, the efficiency of most of the common active pharmaceutical ingredients in commercial drugs are limited in the crystalline state due to low water solubility and dissolution rate (bio-availability), which, instead are enhanced in the amorphous glassy state[2,3]. However, since the advantages of the amorphous formulation are lost upon crystallization, achieving long term stability towards crystallization in the glassy state becomes a key factor for the shelf life of drugs and their controlled delivery into the human body.

According to textbook definitions, glasses are often seen as out-of-equilibrium arrested states, obtained upon cooling a melt under appropriate conditions below the glass transition temperature avoiding the crystallization. Much effort, therefore, has been devoted to the search for coupling between crystallization kinetics and diffusion processes in supercooled liquids. Conversely, it seems that the crystallization kinetics responsible for degradation in pharmaceuticals, biomaterials and food is not directly coupled to diffusive motion, which is strongly inhibited below the glass transition temperature. One possibility, therefore, is that these kinetics are related to other mobility processes active in the arrested state, that ultimately correlate with slow dynamics above T_g[4]. Within this context, fast vibrational dynamics surviving the dynamical arrest occurring in glassy systems can be responsible for long term stability or degradation of pharmaceuticals and, more generally in biological material and food, which often occurs in the amorphous state. Investigations of the mechanical properties of a glass-former across its glass transition are critical to detect any possible fast predictors of the structural arrest which might be embedded in the fast, vibrational dynamics.

Indomethacin (IMC) is an organic glass former with relatively high glass transition temperature T_g= 315 K, interesting for its pharmaceutical application as non-steroidal antipyretic. It has attracted lot of interest as a model system for understanding the stability of amorphous drug formulations. As many pharmaceutical glass-formers, it is characterised by high values of kinetic fragility[5–7] and large tendency towards crystallization even below T_g[8]. Recently, IMC has been used for preparing glasses of

exceptional stability towards crystallization, endowed with low enthalpy, high density and high kinetic stability, by physical vapour deposition[9] with relatively slow deposition rates and controlled substrate temperature.

We report here a study of the mechanical properties, namely the longitudinal modulus and the acoustic loss, of indomethacin, as performed by means of Brillouin light scattering (BLS) at different temperatures, discussing the relationship of the mechanical properties of the supercooled liquid and glass phase. Thanks to its non-destructive capability, this technique provides a unique opportunity to investigate the elastic properties of amorphous pharmaceuticals in general, and to evaluate their kinetic fragility, providing information on the stability of the glass phase.

2 Experimental

High purity indomethacin (IMC) was provided by Sigma-Aldrich. The sample was contained in a 10 mm side square quartz optical cuvette. The cell was flame-sealed under vacuum to avoid any contamination of the IMC powder by oxygen or humidity. The quartz cuvette was placed inside a high temperature thermoresistive furnace, able to thermostate the sample within ± 1 K, from 450 K to room temperature. The required power to set the sample temperature was delivered by a programmable high current power supply, voltage controlled. The BLS measurements were collected approximately every 20 K. Due to the strong absorption of the molten IMC (a brown-yellow liquid), the scattering volume was limited to only 4 to 5 mm of the incoming laser beam, and the scattered intensity was collected through a mininimal thickness of the sample by shifting the laser beam to the side of the cuvette.

Brillouin light scattering is a frequency domain spectroscopy probing thermally excited density fluctuations through the spectrum of scattered light by collective acoustic excitations. For the purposes of the present study, BLS measurements of IMC were collected in the temperature range $298-438$ K, comprising the equilibrium liquid, the supercooled liquid and glassy phase (glass transition T_g = 315 K, melting point T_m = 438 K) at fixed value of exchanged momentum $Q = 4\pi n/\lambda \sin(\theta)$, where n is the refractive index of IMC, λ the probe wavelength and θ half the angle formed by the incident and the scattered light wavevector.

The scattering geometry was the standard 90° setup with the incident beam (514.5 nm line of an Ar^+ laser, operating at an average power of 500 mW) vertically polarized with respect to the scattering plane. The scattered light was collected in a VV polarization configuration, through a linear film polarizer (extinction coefficient $\sim 10^4$). The squared cell geometry allowed scattering to be collected with a minimal stray light.

The spectral analysis of the scattered light was performed using a SOPRA spectrometer[10], especially designed for high resolution and high contrast spectroscopy with visible radiation taking advantages of single pass, double monochromator (model DMDP 2000), based on a fully computerized grating scanning. All the spectra were measured over a frequency shift range extending from -16 GHz to 16 GHz around the excitation frequency. Average integration time of 5 s per point and frequency steps of about 0.13 GHz were used over the entire spectral range for a total acquisition time of about 20 minutes per spectrum, which ensures a very good stability of the overall optical alignments. Each spectral scan was repeated three times. The FWHM resolution obtained using $40-60-60-40$ μm slit widths was 1.6 GHz. The collection solid angle aperture in the scattering plane was kept constant and small enough to reduce the lineshape broadening, due to scattering wavevectors spreading, well below the instrumental resolution.

The refraction index n, necessary to determine the exchanged momentum modulus Q, was taken equal to $n = 1.58$ as reported in literature at $T = 298$ K[11] since the temperature dependence was considered negligible over the probed temperature range accounting for a shift of 4%. Therefore, for the present study, we assumed a constant exchanged momentum $Q \approx 0.0273$ nm^{-1}.

Raw BLS spectra are shown in the left panel of Fig. 1. They are characterized by a central peak with a linewidth ruled by the inverse relaxation time which varies with temperatures by several decades ranging from a few ps in the liquid up to hundreds seconds at the glass transition, signaling the structural arrest. Beside the elastic peak, Brillouin doublet is observed as two symmetrically shifted inelastic components, located at frequency $\pm\nu_0$, defining the phase velocity of the acoustic excitation as $c_s = 2\pi\nu_0/Q = \omega_0/Q$. The Brillouin doublet linewidth provides direct access to the life time of vibrational excitations, i.e. to the acoustic attenuation coefficient $\Gamma(Q)$.

In order to account for the finite experimental resolution of the spectrometer, the BLS spectra have been fitted as the convolution of a Gaussian profile describing the instrumental response and the model function representing the elastic and inelastic components. Where the sound speed c_s and the acoustic attenuation coefficient $\Gamma(Q)$ have been evaluated from the analysis of inelastic components.

As said, BLS probes acoustic modes by phase matching with spontaneous, thermally activated density fluctuations. Acoustic wavepackets, however, can alternatively be stimulated and detected by pump-probe spectroscopies. Among them, broadband

picosecond photoacoustic (BPA), is an experimental technique to coherently generate propagating density fluctuations and subsequently detect them in the time domain through an interferometric approach[12].

BPA measurements were collected by means of an experimental setup whose details are described elsewhere[13,14]. In few words, the output of an ultrashort 800 nm pulsed laser is split in two beams, the pump and the probe. The pump beam is loosely focused on the sample metallic coated substrate to generate a longitudinal acoustic wavepacket by thermal expansion. The acoustic pulse, then, travels inside the sample and its motion is detected by interferometric probing the transient reflectivity $\Delta R/R$ of the femtosecond light probe pulse[12,15]. The oscillating behaviour of the reflectivity as a function of the delay between pump and probe pulses provides relevant information on the acoustic wave travelling in the sample.

For the purpose of the present study, 1.5-2 μm thick glasses of IMC were deposited on a crystalline Si substrate, and a metallic coating on top of the deposition acts as the opto-mechanical transduction medium. The samples temperature was controlled by a liquid nitrogen reservoir cold finger cryostat, coupled with a resistive heater. BPA data were collected in a quasi-backscattering geometry, over a probe continuous spectrum extending from 370 to 730 nm, corresponding to an exchange momentum interval of about $0.025 - 0.049$ nm^{-1}.

3 Results

In a BLS experiment, the spectral response can be modeled (red line in Fig. 1) by the combination of a Lorentzian function for the central peak and the power spectrum of a damped harmonic oscillator (DHO) for the Brillouin doublet, both convoluted with the experimental resolution. This model has been shown to be an appropriate description for glass and supercooled liquid in the hydrodynamic limit[16,17]. A quantum correction accounting for the detailed balance condition is also required. The right panel in Fig.1 shows the pure deconvoluted inelastic spectral component (DHO) as it is obtained by fitting the experimental data at various temperatures. It can be observed that the attenuation, related to the FWHM of the peak, increases with temperature while the acoustic frequency ν_0 related to the peak position, shifts to higher frequencies. As a consequence of the peak frequency shift, the sound speed c_s also increases. The temperature dependencies of the sound speed c_s and of the attenuation Γ normalised by the corresponding ν_0^2 are shown in Fig. 2 and in Fig. 3 respectively. The hypersonic sound velocity exhibits the characteristic sigmoid dispersion curve, limited by the unrelaxed sound velocity c_∞ and relaxed sound velocity c_0, as expected in the presence of the structural relaxation process[18–20]. The kink in c_∞ observed at T_g parts the solid-like velocity in c_∞^{glass} and c_∞^{SCL}, reflecting the structural arrest of the supercooled liquid at the glass transition.

While the BLS signal is proportional to the dynamic structure factor $S(\mathbf{Q},\omega)$, BPA provides direct access to its Fourier transform, the intermediate scattering function $F(\mathbf{Q},t)$. In Fig.4 (upper panel) we show a typical transient reflectivity $\Delta R/R$ time trace, measured in a film of amorphous IMC at $T = 263$ K. In order to evaluate the acoustic frequency ν_0 and the damping $\Gamma(Q)$, we analyzed the differential optical reflectivity oscillations $\Delta R/R$ as function of the time with a damped sine function. Since the signal is probed in the time range 0 - t_{max} = 700 ps, its functional form can be expressed as

$$F(Q,t) = A\, e^{-\pi\Gamma t}[\sin(2\pi\nu_0 t)]\,\Theta(t_{max}-t) \tag{1}$$

where $\Theta(x)$ is the Heaviside step function, and the Q dependence is hidden in the corresponding dependence of the Γ and ν_0 parameters, both depending on the wavelength of the probe pulses.

For a valid comparison with the BLS experimental determinations, then, it is essential to match the isometric condition, i.e. to compare data from the two techniques at the same Q. We then selected a specific wavelength comprised in the broadband white light continuum probe pulse λ_{BPA} in such a way that the corresponding exchanged wavevector Q_{BPA} equals the Q used in the BLS scattering experiment, i.e.

$$Q_{\mathrm{BPA}} = \frac{4\pi}{\lambda_{\mathrm{BPA}}}\sqrt{n(\lambda_{\mathrm{BPA}})^2 - \sin^2(\phi)} = Q_{\mathrm{BLS}} = \frac{2\pi\sqrt{2}}{\lambda_{\mathrm{BLS}}}\, n(\lambda_{\mathrm{BLS}}) = 0.0273\,\mathrm{nm}^{-1} \tag{2}$$

where $\phi = 39^{\mathrm{o}}$, and $n(\lambda)$ is the refraction index of the sample at the given wavelength.

The resulting probe wavelength turns out to be $\lambda_{BPA} \approx 667$ nm. Fig. 4 (lower panel) shows the normalised time Fourier transform of the band pass filtered BPA signal at $\lambda = \lambda_{BPA}$. This spectrum can be fit by the power spectrum of the function $F(Q,t)$. Conveniently, the Fourier transform of a damped sine function wave packet is related to the DHO model, which is its power spectrum, convoluted with a cardinal sine function $\sin(x)/x$ as a result of the limited time extension of the BPA

measurement. The analytic expression of the convolution, used to analyse the spectrum, therefore reads as:

$$S(Q,\omega) = \left| \frac{e^{(-i\omega-\Gamma\pi)t_{max}}[(-i\omega-\Gamma\pi)\sin(2\pi\nu t_{max}) - 2\pi\nu_0\cos(2\pi\nu_0 t_{max})] + 2\pi\nu_0}{(-i\omega-\Gamma\pi)^2 + (2\pi\nu_0)^2} \right|^2 \quad (3)$$

where, as in eq. 1, the Q dependence is hidden in Γ and ν_0. At variance with the BLS response, the BPA spectrum does not show any quasi-elastic peak associated with the structural relaxation: the probed timescale ($t \leq 700$ ps) is much shorter than the structural relaxation time nearby the glass transition. The corresponding sound speed and acoustic attenuation coefficients were evaluated to be 2480.8 ± 2.6 ms^{-1} and 0.245 ± 0.019 GHz respectively. Green symbols in Fig.2 and 3 are related to these BPA determinations.

4 Discussion

Brillouin light scattering measurements of supercooled and glassy IMC exist in literature at temperatures up to 340 K[21]. The resulting sound velocity is reported in Fig. 2 as red symbols, together with our measurements. The agreement shown in Fig. 2 is rather convincing. It is important to remark that the acoustic parameters reported in literature[21] were obtained at a different exchanged momentum ($Q \approx 0.0156 nm^{-1}$) with respect to our BLS experimental conditions.

Differently from the sound velocity c_s, the damping acoustic coefficient Γ heavily depends on the exchanged momentum Q. The acoustic attenuation in disorder systems results indeed from the interplay of different mechanisms, depending on the observed frequency range[22–24]. Therefore, it is interesting to extend our BLS determination of acoustic attenuation to a wider frequency range considering the reported study of vibrational dynamics in the THz regime by inelastic x-ray scattering[25]. The acoustic attenuation coefficient Γ shows an almost quadratic dependence on the frequency ν_0 in the THz regime. In this region wavelengths are comparable to interatomic distances, and the dynamics is dominated by the effects of structural disorder[26]. On the contrary, in the GHz regime anharmonicity effects become relevant and the power dependence exponent of $\Gamma(\nu_0)$ becomes smaller. To emphasize the different dependencies, in Fig. 3 we compare our ν^2-scaled BLS results with inelastic x-ray scattering data. The latter were obtained considering all the measurements at different exchanged momentum Q, i.e. different acoustic frequency ν, and fitting them as $\Gamma = A\nu^2$. The blue symbol corresponds to the parameter $A = 0.679\,10^{-3}$ GHz^{-1}, while the shaded region to its error. To further extend the comparison, we added an additional BLS literature data[21]. As expected, it falls above the smooth decreasing trend of the normalized sound attenuation[18,27] due to the non quadratic dependence of the attenuation in the GHZ region which, however, represent an upper estimate in the absence of Q-dependent BLS data.

In the high-temperature region, the acoustic attenuation, as measured by BLS, is largely due to the presence of the structural relaxation. Below T_g, instead, the structural relaxation is not expected to contribute to the dynamics in the GHz range, being located at lower frequencies. By comparing the BLS acoustic attenuation in the proximity of the glass transition to the IXS unrelaxed data, however, we observe an excess damping. One possibility that has been advanced also in other glass formers (polybutadiene, o-terphenyl and m-toluidin)[18,28–30] is to invoke secondary relaxations, which in IMC has been detected by dielectric relaxation and NMR spectroscopy[31]. On the other hand, it is also true that secondary relaxations in indomethacin are much slower than the timescale probed in this experiment[32]. In view of that, it seems more reasonable to explain the excess damping observed in the proximity of the glass transition based on the nearly constant loss phenomenon as related to the cage dynamics in anharmonic potential. This mechanism is also responsible by the transition observed at T_g for elastic neutron scattering amplitude measured at ps timescale[33].

The fast vibrational dynamics surviving the structural arrest occurring at the glass transition, has been proven to strongly correlate with the slow diffusive dynamics at the supercooled liquid state for a number of diverse systems ranging from strong (as SiO_2) to fragile glasses (as oTP)[34]. The relationship is encoded in the non-ergodicity factor, i.e. the long time limit of the intermediate scattering function $F(Q,t)$ normalised to the static structure factor $S(Q)$:

$$f(Q) = \lim_{t\to\infty} \frac{F(Q,t)}{S(Q)} \quad (4)$$

Specifically, to its low temperature dependence in the $Q \to 0$ limit, quantified by the steepness index α:

$$\alpha = \lim_{Q\to 0} \frac{\mathrm{d}f(Q,T)}{\mathrm{d}T} \quad (5)$$

Within the harmonic approximation for the vibrational dynamics in the glass, the temperature dependence of the non-ergodicity factor in the low Q region follows the analytical dependence:

$$f(Q \to 0, T) = \frac{1}{1 + \alpha \frac{T}{T_g}} \tag{6}$$

and α is determined by the eigenvalues and eigenvectors of the vibrational normal modes. On the other hand, the non-ergodicity factor is also related to the sound velocity jump at the glass transition T_g as:

$$f(Q, T_g) = 1 - \frac{c_0^2(T_g)}{c_\infty^2(T_g)} = 1 - \frac{c_{liquid}^2(T \to T_g^+)}{c_{glass}^2(T \to T_g^-)}. \tag{7}$$

Therefore, according to Eq. 6 and Eq. 7, it follows that

$$\alpha = \left. \frac{c_0^2}{c_\infty^2 - c_0^2} \right|_{T=T_g} \tag{8}$$

providing the way to extract α entirely from the sound velocity temperature dependence measured by BLS across the glass transition.

Remarkably, the parameter α describing the vibrational modes in the glass, deeply correlates with the kinetic fragility $m = \lim_{T \to T_g} \frac{\mathrm{d}\eta}{\mathrm{d}(T_g/T)}$, where the latter describes how fast the shear viscosity η (or the relaxation time $\tau = \eta G_\infty$) changes approaching the glass transition from the liquid side, as the diffusive motion slows down. The correlation observed for glass-former systems with $m < 100$ is linear as:

$$m = \gamma\alpha = (140 \pm 10)\alpha \tag{9}$$

such that the parameter α can be referred to as *glass fragility*.

The kinetic fragility m of IMC has been investigated by different methods[5–7] and it is in the range $60 < m < 79$. Accordingly, IMC is classified as fragile glass-former as the majority of amorphous pharmaceuticals. The corresponding glass fragility, α, of IMC has been recently evaluated by an IXS experiment[25]. Specifically, by isothermal measurement of the non ergodicity factor via the elastic to inelastic scattering ratio, we obtained 0.514, in excellent agreement with the expectations from Eq. 9. By plugging this glass fragility value into Eq.(8), and using the $c_\infty(T_g)$ value from[21], $c_0(T_g)$ can be determined. A further determination of c_0 can be directly obtained by the already mentioned, room temperature IXS study, renormalizing the measured sound velocity by the non ergodicity factor. Both estimates are shown in Fig.2. In absence of ultrasonics data, which would probe the liquid like limit at any temperature above T_g, we report in the same figure $c_0(T)$ assuming the same steepness as $c_\infty^{glass}(T)$. All together, Fig. 2 shows that our data depart from c_∞^{SCL} approaching c_0 at the melting temperature. This is at ease with the expectations from the $\omega\tau \approx 10^{-2} << 1$, having in mind that $\tau \approx 1$ ps in molecular liquids nearby the melting point. Higher temperatures could not be reached due to sample degradation.

5 Conclusions

In conclusion, we have used time and frequency domain Brillouin light scattering for a characterisation of the elastic response of glass-forming indomethacin as function of temperature, from the melting down to the supercooled and glass state. Longitudinal sound velocity and acoustic attenuation have been extracted through the analysis of the Brillouin doublets in the context of hydrodynamic framework with a simple memory function modeling. We tracked the down shift of the mode frequency with temperature, with a characteristic kink occurring near the glass transition and a viscoelastic relaxation towards the liquid-like dynamical regime. The acoustic attenuation displays an increase with temperature across the same range, testifying to the dominance of structural relaxation in the GHz range accessed by BLS.

Our determination of acoustic properties of indomethacin sample extend those previously measured in thin films of IMC by BLS at larger acoustic wavelength[21] around the glass transition temperature, and in bulk ordinary IMC by inelastic x-ray scattering[25] at shorter wavelengths. The comparison requires to consider isometric conditions which for the acoustic attenuation are determined on the assumption of a quadratic dependence on the wave vector. Moreover, we discussed the equivalence of the time domain and frequency domain light scattering techniques, and how the former approach is not able to access to structural relaxations in the glass due to the involved time-scale.

Finally, the measured values of the longitudinal sound velocity and the indirect estimate of the liquid-like asymptotic regime provide support to the correlation of the kinetic fragility, which is believed to represent a key parameter for the stability of amorphous pharmaceuticals[35], with the non ergodicity factor as determined from the sound velocity jump at the glass transition. This result suggests a non-destructive method to asses the kinetic fragility of amorphous pharmaceuticals uniquely from the elastic properties at the glass transition, accessible by inelastic light scattering.

Acknowledgements

T.S. and E.A.A.P. have received funding from the European Research Council under the European Community Seventh Framework Program (FP7/2007-2013)/ERC grant Agreement FEMTOSCOPY No. 207916.

References

1 B. C. Hancock and G. Zografi, *J. Pharm. Sci.*, 1997, **86**, 112.
2 B. C. Hancock and M. Parks, *Pharm. Res.*, 2000, **17**, 397.
3 L. Yu, *Adv. Drug Deliv. Rev.*, 2001, **48**, 27–42.
4 G. Ruocco, F. Sette, R. Di Leonardo, G. Monaco, M. Sampoli, T. Scopigno and G. Viliani, *Phys. Rev. Lett.*, 2000, **84**, 5788–5791.
5 N. T. Correia, J. J. M. Ramos, M. Descamps and G. Collins, *Pharm. Res.*, 2001, **18**, 1767.
6 S. F. Swallen and M. D. Ediger, *Soft Matt.*, 2011, **7**, 10339.
7 J. J. M. Ramos, N. T. Correia, R. Taveira-Marques and G. Collins, *Pharm. Res.*, 2002, **19**, 1879.
8 M. Oshioka, B. C. Hancock and G. Zografi, *J. Pharm. Sci.*, 1994, **83**, 1701.
9 S. F. Swallen, K. L. Kearns, M. K. Mapes, Y. S. Kim, R. J. McMahon, M. D. Ediger, T. Wu, L. Yu and S. Satija, *Science*, 2007, **315**, 353–356.
10 V. Mazzacurati, P. Benassi and G. Ruocco, *J. Phys. E: Sci. Instrum.*, 1988, **21**, 798–804.
11 S. S. Dalal and M. D. Ediger, *Phys. Chem. Lett.*, 2012, **3**, 1229–1233.
12 C. Thomsen, J. Strait, Z. Vardeny, H. J. Maris, J. Tauc and J. J. Hauser, *Phys. Rev. Lett.*, 1984, **53**, 989.
13 E. Pontecorvo, M. Ortolani, D. Polli, M. Ferretti, G. Ruocco, G. Cerullo and T. Scopigno, *Appl. Phys. Lett.*, 2011, **98**, 011901.
14 C. Ferrante, E. Pontecorvo, G. Cerullo, A. Chiasera, G. Ruocco, W. Schirmacher and T. Scopigno, *Nat. Commun.*, 2013, **4**, 1793.
15 A. A. Maznev, K. J. Manke, C. Klieber, K. A. Nelson, S. H. Baek and C. B. Eom, *Opt.Lett.*, 2011, **36**, 2925–2927.
16 J. P. Boon and S. Yip, *Molecular Hydrodynamics*, Courier Dover Publications, 1980.
17 T. Scopigno and G. Ruocco, *Rev. Mod. Phys.*, 2005, **77**, 881–933.
18 L. Comez, C. Masciovecchio, G. Monaco and D. Fioretto, *Progress in Liquid and Glass Physics by Brillouin Scattering Spectroscopy*, Elsevier, 2012, vol. 63, pp. 1–77.
19 F. Scarponi, L. Comez, D. Fioretto and L. Palmieri, *Phis.Rev.B*, 2004, **70**, 054203.
20 G. Monaco, D. Fioretto, L. Comez and G. Ruocco, *Phis.Rev.E*, 2001, **63**, 061502.
21 K. L. Kearns, T. Still, G. Fytas and M. D. Ediger, *Adv. Mat.*, 2010, **22**, 39–42.
22 J. W. S. Rayleigh, *Theory of sound*, Dover Publications, 1976.
23 W. Schirmacher, G. Ruocco and T. Scopigno, *Phys. Rev. Lett.*, 2007, **98**, 025501.
24 W. Schirmacher, B. Schmid, C. Tomaras, G. Viliani, G. G. Baldi, G. Ruocco and T. Scopigno, *Phys. Stat. Sol.(c)*, 2008, **3**, 862–866.
25 E. A. A. Pogna, C. C. Rodriguez-Tinoco, M. Krisch, J. Rodriguez-Viejo and T. Scopigno, *Sci. Rep.*, 2013, **3**, 2518.
26 F. Sette, M. H. Krisch, C. Masciovecchio, G. Ruocco and G. Monaco, *Science*, 1998, **280**, 1550.
27 C. Tomaras, B. Schmid and W. Schirmacher, *Phys. Rev. B*, 2010, **81**, 104206.
28 L. Comez, D. Fioretto, G. Monaco and G. Ruocco, *J. Non-Cryst. Solids*, 2002, **307-310**, 148153.
29 L. Comez, M. Pietrella, D. Fioretto, G. Monaco, F. Scarponia, R. Verbeni and L. Palmieri, *Philos. Mag.*, 2007, **87**, 651–656.
30 K. Herzfeld and T. Litovitz, *Absorption and Dispersion of Ultrasonic Waves*, Academic Press, New York, 1959.
31 L. Carpentier, R. Decressain, S. Desprez and M. Descamps, *J. Phys.Chem. B*, 2006, **110**, 457–464.

32 S. Capaccioli, K. L. Ngai, M. Paluch and D. Prevosto, *Phys. Rev. E*, 2012, **86**, 051503.
33 S. Capaccioli, K. L. Ngai, S. Ancherbak and A. Paciaroni, *The Journal of Physical Chemistry B*, 2012, **116**, 1745–1757.
34 T. Scopigno, G. Ruocco, F. Sette and G. Monaco, *Science*, 2003, **302**, 849.
35 S. Yoshioka and Y. Aso, *J. Pharm. Sci.*, 2007, **96**, 960–981.

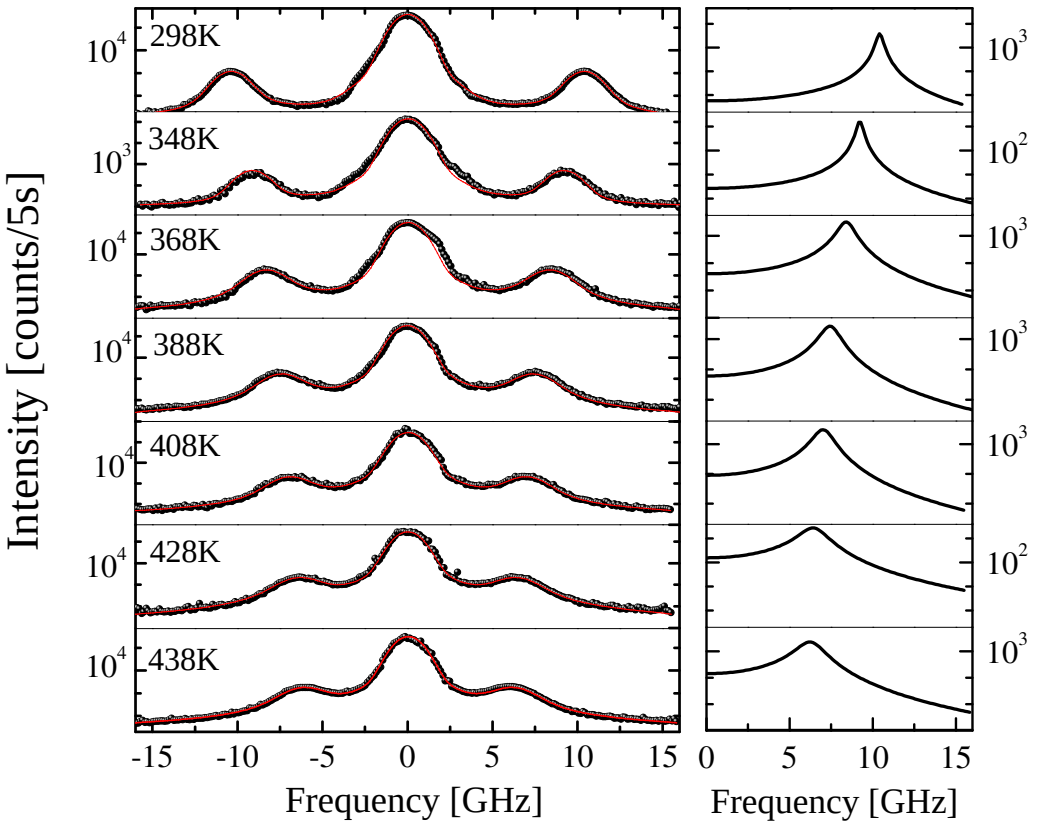

Fig. 1: Left panel: Brillouin light scattering spectra of supercooled bulk indomethacin at fixed exchanged momentum $Q = 0.0273$ nm^{-1} (circles: experimental points; continuous red line: best fit). Data are vertically shifted for different temperatures. The experimental error is within the symbol. Right panel: deconvoluted DHO components as determined by fitting the experimental data.

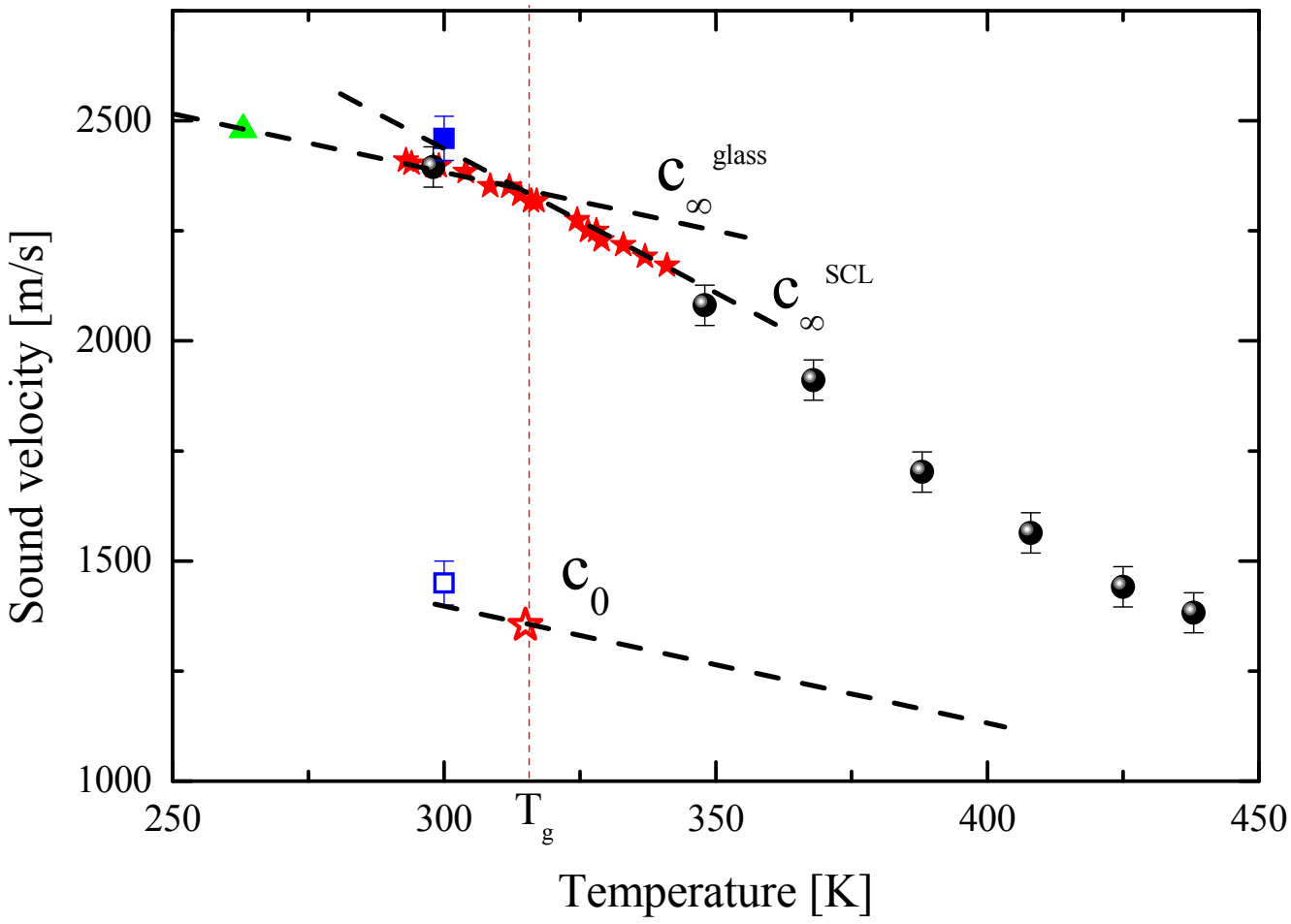

Fig. 2: Sound velocity, c_s, of indomethacin as a function of temperature T. BLS data (black symbols) are extracted from the spectra of Fig. 1, while the BPA value (green triangle) is related to the time trace in Fig. 4. Previous literature data are reported in red[21]. An Inelastic x-ray scattering determination[25] is also reported (blue square). Liquid-like values of the sound velocity, c_0, around T_g have also been determined through the procedure explained in the text. The dashed lines indicate the liquid, supercooled liquid and glass sound velocity limits.

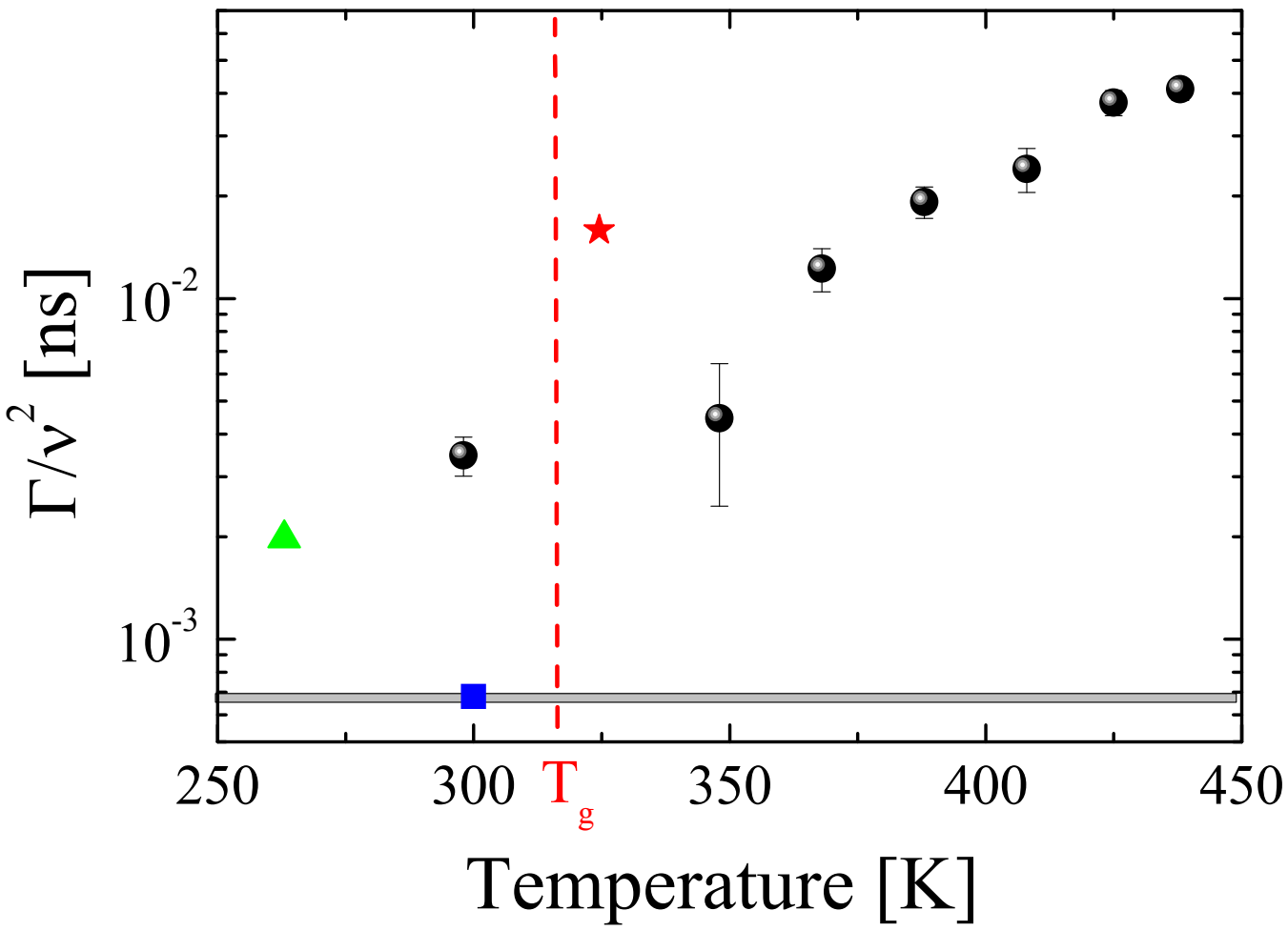

Fig. 3: Acoustic attenuation coefficient Γ of indomethacin, normalised to square frequency $\nu = \omega_0/(2\pi)$, as a function of temperature T. Black symbols are obtained from the fit of BLS spectra in Fig. 1. Green triangle is referred to BPA data, shown in fig 4. An Inelastic x-ray scattering determination, obtained in the Thz range at different exchanged momentum Q[25] is also reported, with a grey region indicating the error (no significant temperature dependence is expected at such high frequencies[18]). Red symbol indicates a BLS datum available in literature for acoustic attenuation (see Fig. 3a in[21]), but for an exchanged momentum ($Q \approx 0.0156$ nm^{-1}), i.e. lower than that reported here.

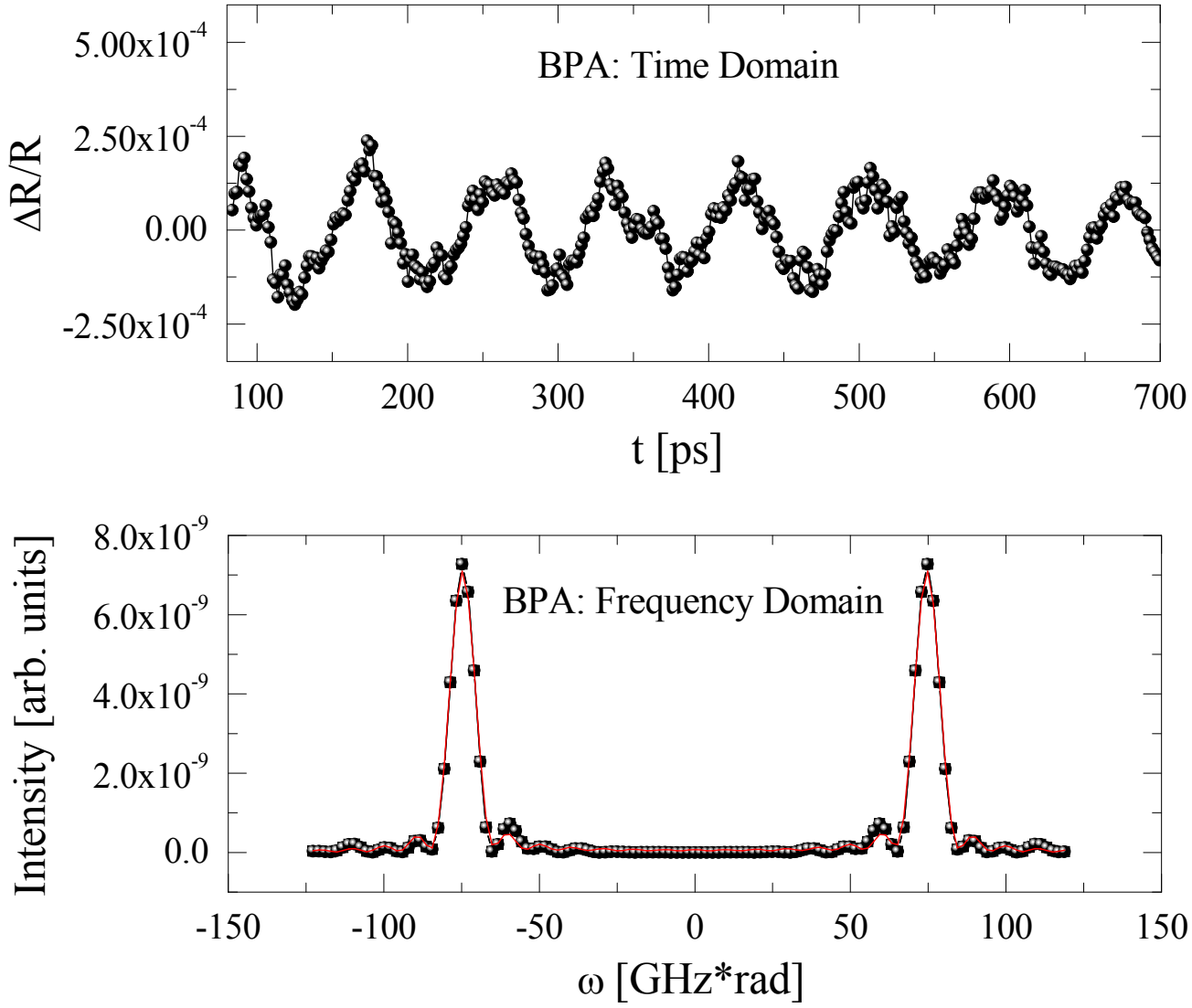

Fig. 4: Upper panel: differential optical reflectivity of indomethacin as a function of time delay at $\lambda_{probe} = 666.8$ nm at $T = 263$ K, detected by BPA. A slow decaying thermal contribution has been subtracted by the original trace to account for electron driven heat diffusion. Furthermore, the trace has been smoothed, using a moving average, binning over 13 adjacent time values. Lower panel: Fourier transform of the original trace in frequency domain. Data have been fitted (red line), as described in the text.

Brillouin light scattering and broadband picosecond photoacoustic experiments measure the elastic response of Indomethacin from the melting point to the glass transition through the undercooled liquid phase.